Experimental photoluminescence and lifetimes at wavelengths including beyond 7 microns in Sm^{3+}-doped selenide-chalcogenide glass fibers.

Richard W. Crane[1,*], Łukasz Sójka[2,*], David Furniss[1], Joel Nunes[1], Emma Barney[1], Mark C. Farries[1], Trevor M. Benson[1], Slawomir Sujecki[1] and Angela B. Seddon[1].

[1]*Mid-Infrared Photonics Group, George Green Institute for Electromagnetics Research, Faculty of Engineering, University Park, University of Nottingham, Nottingham, NG7 2RD, UK.*
[2]*Telecommunications and Teleinformatics Department, Wroclaw University of Technology, Wybrzeze Wyspianskiego 27, 50-370, Wroclaw, Poland.*
emxrc1@exmail.nottingham.ac.uk;lukasz.sojka@pwr.edu.pl;angela.seddon@nottingham.ac.uk

Abstract: 1000 ppmw Sm^{3+}-doped $Ge_{19.4}Sb_{9.7}Se_{67.9}Ga_3$ atomic % chalcogenide bulk glass and unstructured fiber are prepared. Near- and mid-infrared absorption spectra of the bulk glass reveal Sm^{3+} electronic absorption bands, and extrinsic vibrational absorption bands, due to host impurities. Fiber photoluminescence, centred at 3.75 μm and 7.25 μm, is measured when pumping at either 1300 or 1470 nm. Pumping at 1470 nm enables the photoluminescent lifetime at 7.3 μm to be measured for the first time which was ~100 μs. This is the longest to date, experimentally observed lifetime in the 6.5-9 μm wavelength-range of a lanthanide-doped chalcogenide glass fiber.

1. Introduction:

The mid-infrared (MIR) region (3-50 μm wavelength range) [1] houses the fundamental vibrational absorption bands of molecules. MIR light sources of sufficient power output would enable the real-time detection of target molecules, an attractive prospect for a variety of industries and the environmental, food and drink, fossil fuel, defense and medical sectors [2]. Walsh *et al.* [3] have recently compared the attributes of both currently available and future potential MIR laser sources. They emphasized the advantages of active lanthanide-doped MIR solid-state lasers, of: high power, or energy, output; narrow spectral linewidth; a wide variety of pulse widths and pulse repetition rates; broad tunability; efficient operation *via* direct diode laser pumping and excellent beam quality. Lanthanide-doped MIR solid-state *fiber* lasers have the added potential advantages of diffraction-limited output and compactness. With medical applications in mind, then lanthanide-doped MIR solid-state fiber lasers have the potential to operate at wavelengths between 6-9 μm and so be resonant with the so-called amide I, II and III tissue absorption bands at wavelengths: 5.90-6.15 μm (due to C=O of amide); ~6.45 μm (N-H, C-H) and 7.63-8.33 μm (N-H, C-H), respectively, [4] with the capacity to provide a new generation of precision surgical lasers [5] to potentially minimise collateral damage to surrounding tissue. In addition, lanthanide-doped MIR solid-state fiber lasers operating as pulsed lasers in the MIR spectral region are needed in the wavelength range 4-7 μm for pumping chalcogenide glass fiber MIR supercontinuum lasers, to enable a compact, all-fiber solution, for use in MIR endoscopic probes to provide *in vivo* chemical mapping of tissue for disease diagnostics [6,7].

To achieve such longer wavelength lanthanide-doped MIR solid-state fiber lasers, a low phonon energy host is prerequisite [8, 9]. Er^{3+}-ZBLAN, and Ho^{3+}-InF_3, fibers have been demonstrated to lase at room temperature at 3.78, and 3.92 μm, respectively, [10, 11]. This probably represents the long wavelength limit of laser operation beyond which the phonon energy of these host matrices favours non-radiative emission.

Within a sulfide fibre matrix ($Ga_5Ge_{20}Sb_{10}S_{65}$ at. %) , the simultaneous luminescence of both Pr^{3+} (fixed:1000 ppmw) and Dy^{3+} (between 200 and 1000 ppmw) has been reported to give rise to broad continuous photo-luminescence across the 2.2–5.5 μm wavelength range, which was used for mid-infrared fibre gas sensing of CO_2 and CH_4 [12]. Also, $Ga_5Ge_{20}Sb_{15}S_{60}$ at. % bulk glasses doped with 1000 to 10,000 ppmw Dy^{3+} have been purified, fibreised and characterised [13].

Selenide-based chalcogenide fibers, on the other hand, present lower phonon energies than the sulfides of 250-300 cm^{-1} and display a large low-loss transmission window (~1-10 μm) with lowest intrinsic loss around 5.5-6.5 μm [8]. GeSbGaSe host glasses have been shown to support radiative transitions emitting out to 8 μm in a Tb^{3+} doped chalcogenide composition [14]. Despite this, no MIR lasing has yet been recorded in chalcogenide fiber. Fabrication of such glass fibers requires careful purification to exhibit low concentrations of extrinsic impurities like: oxygen, hydrogen, carbon, and silica, and be free of devitrification.

Samarium (III) has been identified as a potential candidate for providing MIR lasing in the 3-4 μm (*e.g.* $^6H_{11/2}$ to $^6H_{7/2}$) and 6-8 μm region (*e.g.* $^6H_{11/2}$ to $^6H_{9/2}$) [3]. Recent work has shown that a 1000 ppmw Sm^{3+} doped $Ge_{20}Sb_{10}Se_{65}Ga_5$ atomic % (at. %) fiber was capable of emission from 6.5-8.5 μm; although no lifetime measurements were reported for this long wavelength emission, an 11 μs time decay constant was reported at both 3.7 μm and 1.95 μm wavelengths [15]. Earlier work on Sm^{3+} doped chalcogenide glasses focused on their near-infrared (NIR) PL behaviour [16] and indeed a visible emission, Sm^{3+}-oxide glass fiber laser was previously reported in the 1980s [17].

The work presented in this Paper details the development of a $(GeSbSe)_{97}Ga_3$ at. % glass doped with 1000 ppmw Sm^{3+} which was drawn to fiber. MIR bulk absorption spectra, fiber optical loss, photoluminescence (PL) and PL lifetimes are presented. Here, we report the longest to date, experimentally observed, photoluminescence lifetime of ~ 0.1 ms for a lanthanide ion doped chalcogenide glass fiber, within the 6.5-9 μm range.

2. Methods:

2.1. Bulk glass and fiber preparation

The $Ge_{19.4}Sb_{9.7}Se_{67.9}Ga_3$ at. % glass (code: M227RERC) doped with 1000 ppmw Sm^{3+} was melted and drawn to fiber (code: F099RERC). Ge (5N, Materion), Sb (6N, Materion), Se (5N, Materion), and Ga (7N, Alfa Aesar) were batched in a N_2 atmosphere MBraun glove box (<0.1 ppm H_2O, <0.1 ppm O_2) into an air/vacuum baked silica glass ampoule (<0.1 ppm OH, Multilab). This ampoule was sealed under vacuum (10^{-3} Pa) and the batch melted at 900 °C /12 hours. The melt was quenched and annealed at the DSC (differential scanning calorimetry) onset glass transition temperature (T_g) [18]. The ampoule was returned to the glovebox; 1000 ppmw Sm (3N, Alfa Aesar) was batched-on and the ampoule resealed under vacuum and heated to 900 °C for a further 2 hours, before identical quenching/ annealing. The preform was drawn to unstructured fiber, of ~ 400 μm diameter (413-418 um over 185 mm length) on a modified Heathway fiber-draw tower housed in a class-10,000 clean room.

2.2 Near-infrared (NIR) and mid-infrared (MIR) absorption spectra of bulk Sm^{3+}-doped selenide-chalcogenide glass

NIR and MIR absorption spectra of bulk, 1000 ppmw Sm^{3+}-doped $(GeSbSe)_{97}Ga_3$ at. % glass were collected from a sample cut from the annealed glass rod, then ground and polished to a 1 μm finish, to form a 10 mm diameter, 2.74 mm optically thick disc. Spectra were collected using a Fourier transform infrared spectrometer (FTIR; IFS 66/S, Bruker), purged with air (H_2O and CO_2 removed) and equipped with a DTGS (deuterated triglycine sulfate) detector. A W lamp source was used with CaF_2 beam splitter for 1-2.5 μm operation and Globar© light source with KBr beam splitter for the 2.5-10 μm range.

2.3 MIR optical loss of fiber

Optical loss of the 1000 ppmw Sm^{3+}-doped $(GeSbSe)_{97}Ga_3$ at. % glass fiber in the 3-9 µm wavelength range was measured using the cut-back method. The IFS 66/S, Bruker FTIR was used with purging air, as above, and a GloBar© blackbody source, KBr beamsplitter and liquid N_2 cooled indium antimonide (InSb, InfraRed Associates Inc.) and mercury-cadmium-telluride (MCT, Kolmar Technologies: V100-1B-7) detectors, to cover the NIR and MIR spectral regions, respectively. Further measurement details may be found in [19].

2.4 Photoluminescence (PL) intensities and lifetimes

2.4.1 Fiber-end-collection of PL intensities

1000 ppmw Sm^{3+}-doped $(GeSbSe)_{97}Ga_3$ at. % glass fiber of 75 mm length and 415 ± 3µm diameter was end-pumped (see Fig. 1) and the PL intensity detected at around 2.7, 3.7 and 7.3 µm wavelength, as detailed below.

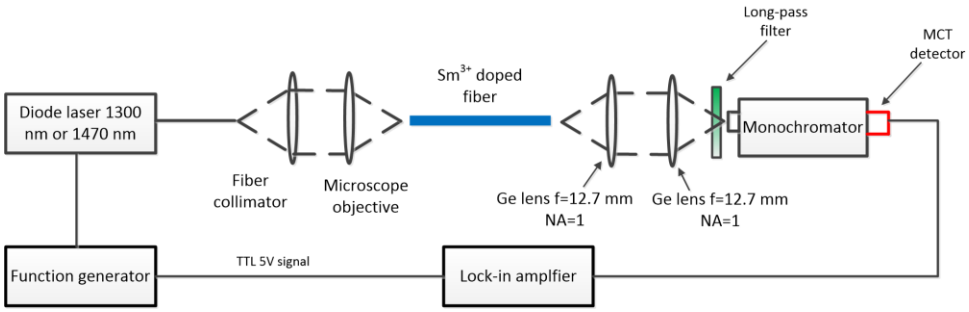

Fig. 1. Fiber-end-collection set-up for measurement of PL intensity at *ca.* 2.7, 3.7 and 7.3 µm wavelengths from the 1000 ppmw Sm^{3+}-doped $(GeSbSe)_{97}Ga_3$ glass fiber of 75 mm length and 415 ±3 µm diameter.

Sm^{3+} ions doped in the selenide-chalcogenide glass fiber host were excited by either a 1470 nm laser diode (SemiNex: 4PN-127) or 1300 nm laser diode (SemiNex: 4PN-116). The pump laser beams were chopped in order to reduced thermal background noise from the sample, optical elements and other laboratory equipment. For example, the remaining pump power exiting the fiber-end, opposite to that pumped, heated a long-pass filter, down- circuit (Fig. 1 and see below) and produced thermal background noise. Chopping the pump laser beam meant not only that the absolute heat load of the sample was reduced, but also that blackbody radiation from sample, optical components and *etc.* was reduced as it was not modulated by the chopper. Thus, the pump beam was electronically chopped by means of a function generator (GW INSTEK GFG-3015) of low frequency, ~20 Hz; the chopping period of 50 ms was chosen to be long compared to the Sm^{3+} MIR PL life-times (~100 µs, see Section 3).

The resulting PL emission, from the fiber end opposite to that pumped (Fig. 1), was focused through a pair of Ge aspheric lenses (Edmund Optics: code 89-607, AR (anti-reflection coated) for 3-12 µm wavelength range), each of NA (numerical aperture): 1, and focal length: 12.7 mm. Lenses of short focal length/high NA were best suited for efficient collection of the fiber PL, and selected to match the high refractive index (n) of the unstructured chalcogenide glass fiber (*e.g.* n ~2.55 at 3-10 µm, for undoped $Ge_{20}Sb_{10}Se_{70}$ at. % [20]) and high fiber NA (>>1). This approach was instigated at the Wrocław University of Technology and has been used in [21]. The Ge lens pair also acted as a 2 µm long-pass filter, thus any residual pump signal exiting the fiber-end was eliminated before reaching the next long-pass filter and monochromator further along the optical circuit (see Fig. 1, and below).

The PL exiting the fiber, resulting from excitation with the 1300 or 1470 nm laser diode, was first directed through the Ge lens pair, then passed through a long-pass filter of cut-on wavelength 3 µm (Spectrogon: 71M09339) into a monochromator (MSH-150, Quantum Lot (focal length: 150 mm), calibrated by Bentham in 2018) operating with a 4000 nm blazed, 150 line/ mm grating and onto the detector. Detection of the signal was achieved with a thermoelectric cooled (200 K) MCT (mercury cadmium telluride) detector (Vigo System: PVI-4TE-8), operating in the spectral range: 3 µm to 9 µm.

Additionally, the thermoelectric cooled (200 K) MCT (Vigo System: PVI-4TE-5) was used operating in the spectral range: 2 µm to 6.0 µm. The PL exiting the fiber, resulting from excitation with the 1300 or 1470 nm laser diode, was directed through the Ge lens pair, then passed through a long-pass filter of cut-on wavelength 6.15 µm (Spectrogon: 71M09001) then into the same monochromator as above, but operating with a 9000 nm blazed, 100 line/ mm grating, and then onto the same MCT detectors as above. All measured spectra were corrected for system response

2.4.2 Fiber-side-collection of PL lifetimes

For the PL lifetime measurements, the 1000 ppmw Sm^{3+}-doped $(GeSbSe)_{97}Ga_3$ at. % fiber (code:F099RERC) of diameter 415 ±3 µm was end-pumped with modulated light from the pump laser at 1470 nm.

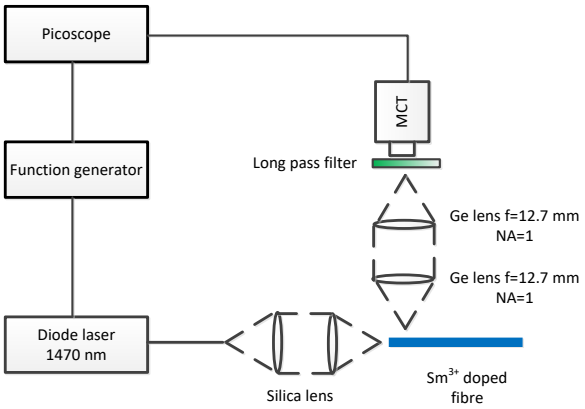

Fig. 2. Fiber side-collection set-up for measurement of PL lifetimes at *ca.* 3.7 and 7.3 µm wavelength from the 1000 ppmw Sm^{3+}-doped $(GeSbSe)_{97}Ga_3$ glass fiber of 415 ±3 µm diameter pumped at 1470 nm wavelength.

A function generator (GW INSTEK GFG-3015) coupled to laser diode drivers (Thorlabs: LBC240C) was used to produce a square-wave signal, which modulated the laser diode, switching it on and off. The resultant periodic PL excitation from the fiber under the side emission set-up (Fig. 2), and close to the pumped fiber end, was then directed through the pair of Ge lenses and through the long-pass filter (cut-on at 3 µm or 6.15 µm) into the MCT detector. The MCT detector was used to measure the intensity decay of the fiber PL side-emission. The signal from the MCT photodetector was directed to an oscilloscope. In order to suppress noise, averaging over several thousand excitation processes was performed several times.

For lifetime measurement at nominally 3.75 µm wavelength, the 3 µm cut-on filter and MCT photodetector (Vigo System PVI-4TE-5, operation: 2-6 µm) were used. This detector and preamplifier together have a quoted bandwidth of 17 MHz (rise time 20 ns). For the lifetime measurement nominally at 7.25 µm wavelength, the 6.15 µm cut-on filter and second MCT detector (Vigo System PVI-4TE-8: operation: 3-9 µm) was used. The detector quoted bandwidth with preamplifier was 150 kHz, with a rise time of 2 µs.

3. Results

3.1 Sm doped bulk GeSbSeGa glass absorption

Fig. 3 shows absorption spectra of the 1000 ppmw Sm^{3+}-doped $(GeSbSe)_{97}Ga_3$ atomic % chalcogenide bulk glass across: (a) 1-2.2 µm wavelength span and (b) 2-10 µm. Table 1 lists the observed wavelength positions and assignment of Sm^{3+} $^6H_{5/2}$ ground-state to excited state transitions; assignments were compared with those of other authors *viz.:* Starecki *et al.* [15] for (500 or 1000 ppm, unstated) Sm^{3+}-doped $Ga_5Ge_{20}Sb_{10}Se_{65}$ at. % bulk glass and Němec *et al.* [16] for $Sm_2Se_3)_{0.5}(Ge_{30}Ga_5Se_{65})_{99.5}$ molar ratio, bulk glass.

Fig. 3(b) shows extrinsic impurity vibrational absorption bands and Sm^{3+} electronic absorptions in the 2-9 µm region; their interpretation is now discussed. From MIR spectra of bulk undoped $Ge_{20}Sb_{10}Se_{70}$ at. % glasses, similar to the host glass here [22], the single strong vibrational absorption band centred at 2.8-2.9 µm was assigned as [O-H] and thus

the adjacent 2.65 μm, strong, absorption band, missing in undoped glasses [22], was assigned as to Sm^{3+}: $^6H_{5/2} \rightarrow {}^6H_{11/2}$ (*cf.* 2700 nm expected [16], Table 1). Also, from MIR spectra of bulk undoped $Ge_{20}Sb_{10}Se_{70}$ at. % glasses [22], the strong band at 4.6 μm may be assigned as [H-Se] extrinsic absorption; a much smaller [H-Se] band was also expected at 4.1 μm [22]. Therefore, it is tentatively suggested that the Sm^{3+} transition: $^6H_{5/2} \rightarrow {}^6H_{9/2}$ manifests in Fig. 3(b) as the small shoulder at 4.30 μm (*cf.* 4500 nm expected [16], Table 1).) and that the 4.1 μm [H-Se] has been artificially inflated in Fig.3(b) in intensity due to its wavelength proximity to the large 4.30 μm Sm^{3+} band. Finally, the absorption band at 9.58 μm is assigned to the Sm^{3+}: $^6H_{5/2} \rightarrow {}^6H_{7/2}$ electronic absorption band (*cf.* 9600 nm expected [16], Table 1). Note that the underlying optical loss of similarly purified, but undoped, fiber was ~4 dB/m [22] at 10 μm wavelength.

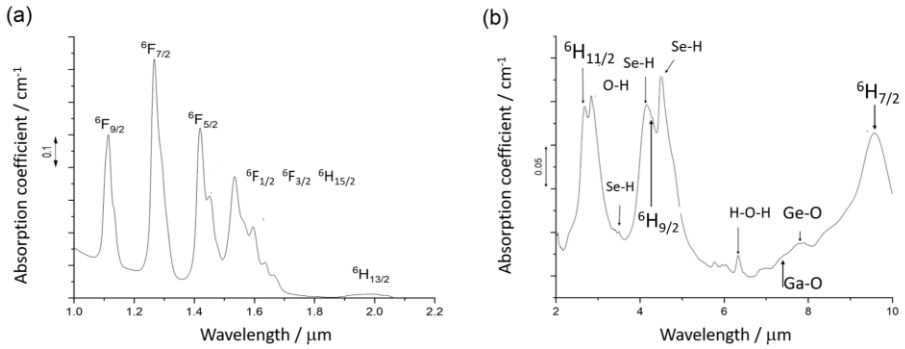

Fig. 3. MIR absorption spectra of bulk 1000 ppmw Sm^{3+}-doped $(GeSbSe)_{97}Ga_3$ glass spanning: (a) the NIR and (b) the NIR to MIR.

Table 1. Wavelength positions and transition assignments of Sm^{3+} electronic absorption bands observed here (see Fig. 3) for transitions from the ground state: $^6H_{5/2}$, up to excited states. Assignments are compared with those of: Starecki *et al.* [15] for (500 or 1000 ppm, unstated) Sm^{3+}-doped $Ga_5Ge_{20}Sb_{10}Se_{65}$ at. % bulk glass and Němec *et al.* [16] for $(Sm_2Se_3)_{0.5}(Ge_{30}Ga_5Se_{65})_{99.5}$ molar ratio, bulk glass.
Key: wk is weak, br is broad, sh is sharp, v is very.

Observed in this work. Peak wavelength / nm, for transition from $^6H_{5/2}$ to:	**Observed in [16]. Peak wavelength / nm, for transition from $^6H_{5/2}$ to:**	**Observed in [15]. Peak wavelength / nm, for transition from $^6H_{5/2}$ to:**
9580 (strong) $^6H_{7/2}$	9600 (expected, not measured).	Not measured.
4300 (strong) $^6H_{9/2}$	4500 (expected, not measured).	Not measured.
2650 (strong) $^6H_{11/2}$	2700 (expected, not measured).	Not measured.
2000 (wk, br) $^6H_{13/2}$ (tentative)	2000 (wk, br) Not identified	1970 (wk br) $^6H_{13/2}$
1670 (wk, br shoulder). See*	~1675 (wk, br shoulder). See*	1675 (wk br shoulder). $^6F_{1/2}$
1630 (wk, sh shoulder). See*	1630 (wk, sh shoulder). See*	1630 (wk, sh shoulder) Not identified.
1600 (wk, sh shoulder). See*	1600 (wk, sh shoulder). See*	1595 (wk, sh shoulder). $^6F_{3/2}$
1570 (v wk, br shoulder). See*.	1570 (v wk, br shoulder). See*	1570 (v wk, br shoulder). Not identified.
1530 (strong) (*authors suggest encompasses 1570, 1600, 1630, 1670) $^6F_{1/2}$ $^6F_{3/2}$ $^6H_{15/2}$	1528 (strong), (*authors imply covers 1570, 1600, 1630, 1675) $^6F_{1/2}$ $^6F_{3/2}$ $^6H_{15/2}$	1530 (strong) $^6H_{15/2}$
1440 (wk sh shoulder) Not identified.	1430 (wk sh shoulder) Not identified.	1450 (wk br shoulder) Not identified.
1420 (strong) $^6F_{5/2}$	1414 (strong) $^6F_{5/2}$	1425 (strong) $^6F_{5/2}$
1260 (strong) $^6F_{7/2}$	1262 (strong) $^6F_{7/2}$	1270 (strong) $^6F_{7/2}$
1110 (strong) $^6F_{9/2}$	1108 (strong) $^6F_{9/2}$	1120 (strong) $^6F_{9/2}$
Not measured.	966 $^6F_{11/2}$	Not measured.

Extrinsic vibrational absorption bands due to unwanted oxide contamination ([Sb-O], [Se-O], [Ga-O]) are expected to lie >10 µm wavelength, except [Ga-O] is reported to absorb also at 7.3 µm [23]. Extrinsic vibrational bands due to [H-O-H], [Ge-O] and [Ga-O] are observed at 6.3 µm [24], 7.83 µm [25] and 7.25 µm [23], respectively. Note also that absorption bands at 2.8-2.9 µm and 6.3 µm are likely exacerbated by atmospheric absorptions unrelated to the glass, despite a dry air purging system being in place.

From Fig. 3 and Table 1, from a practical point of view, Sm^{3+} exhibits many absorption bands for pumping using commercially available laser diodes and fiber lasers.

3.2 Fiber optical loss

Fig. 4 shows the MIR optical loss spectrum of the 1000 ppmw Sm^{3+}-doped $(GeSbSe)_{97}Ga_3$ unstructured glass fiber. The ~4-5 µm region has been omitted due to large absorption (see Fig. 3(a)). The lowest loss in this fiber was 2.15 dB/m at 6.04 µm.

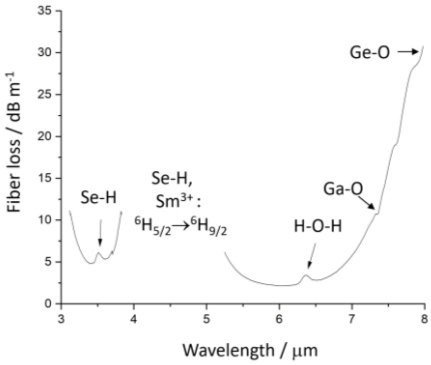

*Fig. 4. MIR optical loss of 1000 ppmw Sm^{3+}-doped $(GeSbSe)_{97}Ga_3$ glass fiber in the 3-9 µm range. Extrinsic vibrational absorption bands due to the presence of unwanted host glass impurities are identified and Sm^{3+} ground-state electronic absorption (*see also *Fig. 3(b)and Table 1). (4-5 µm omitted due to strong absorption.)*

3.3 Fiber photoluminescence

3.3.1 PL centred at 3.75 µm and 7.25 µm

(i) PL at 3.75 µm (end-pumping at 1470 nm / 300 mW or 1300 nm / 350 mW)

75 mm of unstructured 1000 ppmw Sm^{3+}-doped $(GeSbSe)_{97}Ga_3$ fiber, 415 ±3 µm diameter, was investigated for PL at nominally 3.75 µm (expected due to $^6H_{13/2} \rightarrow {}^6H_{9/2}$ transition) from the fiber-end opposite that end-pumped with 1470 nm at 300 mW or 1300 nm at 350 mW (Fig. 1) with cut-on filter at 3000 nm. This transition was reported to have a relatively high branching ratio of ~ 0.33 [15] from Judd-Ofelt modelling, and was more simple to detect than PL >7 µm (see section 3.3.1(ii)). The initially low signal, centered at 3.75 µm, was improved with optimal optical alignment. Measurement parameters were: MCT detector (Vigo, PVI-4TE-8 (3 µm-9 µm); lock-in amplifier: sensitivity 30 mV, time-constant 300 ms; monochromator software: time averaging: 3 s.

Figure 5(a) shows normalised emission spectra in the 3.25-4.5 µm wavelength range when pumped with 350 mW at 1300 nm, or 300mW at 1470 nm. The slight decrease in intensity at around 4.25 µm was attributed to atmospheric CO_2 absorption. From Fig. 5(a), the spectral shape and central wavelength are in good agreement with the results of Starecki *et al.* [15].

(ii) PL at 7.25 µm (end-pumping at 1470 nm / 300 mW or 1300 nm / 350 mW))

75 mm long of unstructured 1000 ppmw Sm^{3+}-doped $(GeSbSe)_{97}Ga_3$ fiber of 415 ±3 µm diameter was investigated for PL at nominally 7.25 µm (expected due to the $^6H_{13/2} \rightarrow {}^6H_{11/2}$ transition) from the fiber-end opposite that end-pumped with 1470 nm at 300 mW or 1300 nm at 350 mW (Fig. 1) with cut-on filter at 6150 nm. This transition was reported to have a relatively low branching ratio of ~ 0.08 [15] from Judd-Ofelt modelling, and was more difficult to detect than the ~3.75 µm wavelength emission.

From Fig. 5(b), PL centered at 7.25 µm, had spectral shape and central wavelength in good agreement with results in [15]. The 6150 nm cut-on filter caused an abrupt PL onset at ~ 6230 nm. From the observed PL bandshape (Fig. 5(b)), the 6–9 µm emission band appeared to be mainly associated with the $^6H_{13/2} \rightarrow {}^6H_{11/2}$ transition, expected at 7.18 µm [15]. However, we suggest also that emission from $^6H_{11/2} \rightarrow {}^6H_{9/2}$, expected at 7.77 µm [15], with the same branching ratio of 0.08 as the larger gap transition: $^6H_{13/2} \rightarrow {}^6H_{11/2}$ [15], did contribute to this MIR emission, despite its small energy gap.

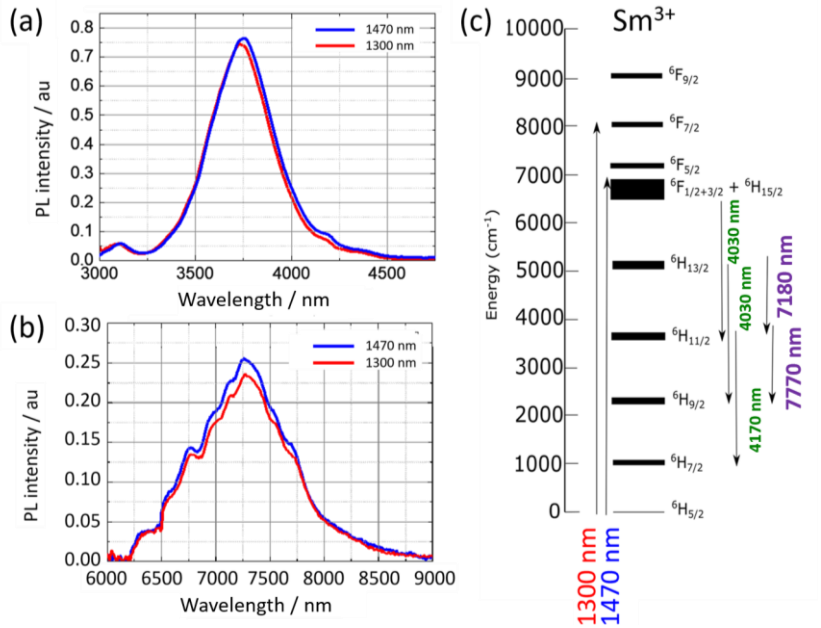

Fig. 5. (a) and (b) Photoluminescence spectra of the 1000 ppmw Sm^{3+}-doped $(GeSbSe)_{97}Ga_3$ glass fiber, pumped at 1470 nm wavelength with 300 mW (upper (blue) curve at peak wavelength, in each case (a) and (b)) or pumped at 1300 nm wavelength with 350 mW. Fiber-end collection of the PL was applied. PL was centered at 3750 nm and 7250 nm in (a) and (b), respectively. (c) Energy level diagram of Sm^{3+}, indicating pump absorption transitions and emission transitions contributing to spectra in (a) and (b).

3.3.2 PL at 2.7 µm (end-pumping at 1470 nm / 300 mW)

75 mm of 415 ±3 µm diameter, unstructured 1000 ppmw Sm^{3+}-doped $(GeSbSe)_{97}Ga_3$ fiber was investigated for <3 µm PL, by end-pumping at 1470 nm / 300 mW. A MCT detector (operating: 2-6 µm) was used with the Ge lens pair (Fig. 1) acting as a 2 µm long-pass filter. The measured spectrum was calibrated for system response. Emission associated with Sm^{3+}: $^6H_{13/2} \rightarrow {}^6H_{7/2}$ centered at 2.59 µm (high branching ratio: 0.42 [15]) was expected to dominate. Both $^6H_{11/2} \rightarrow {}^6H_{5/2}$ centered at 2.85 µm (high branching ratio: 0.56 [15]) and ($^6F_{1/2}$, $^6F_{3/2}$, $^6H_{15/2}$) $\rightarrow {}^6H_{9/2}$ centered at 2.65 µm (low branching ratio: 0.18 [15]) may contribute. From Fig. 6, PL was observed from 2250-3200 nm, centred at 2.7 µm. This result partially confirms non-quenching of the transition $^6H_{11/2} \rightarrow {}^6H_{5/2}$ as PL was observed at~ 2.8 µm, contrary to the prediction in [15].

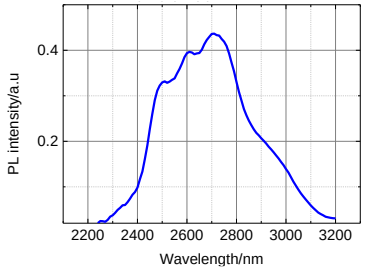

Fig. 6. Photoluminescence spectrum of the 1000 ppmw Sm^{3+}-doped $(GeSbSe)_{97}Ga_3$ glass fiber (75 mm long and 415 ±3 µm diameter). The fiber was end pumped at 1470 nm wavelength with 300 mW power. Fiber-end collection of the PL was applied and the spectrum was corrected for system response.

3.4 Fiber photoluminescent lifetimes

(i) PL decay centered at 3. 75 µm, cut-on filter at 3.00 µm, fiber-side collection

Fig. 7 presents PL decay of the 1000 ppmw Sm^{3+}-doped $(GeSbSe)_{97}Ga_3$ glass fiber measured using a MCT detector (PVI-4TE-5) and cut-on filter at 3.00 µm. PL was centered at 3.75 µm (see Fig. 5(a)). As low pump power as possible was used to minimise sample heating. The decay was measured from the fiber-side. Measurements were repeated three times: 0.100 ms, 0.102 ms and 0.101 ms. A single exponential was applied (*e.g.* see Fig. 7) but it was not possible to achieve a perfect fit. It is suggested that this PL lifetime was due to a combination of two transitions: $^6H_{13/2} \rightarrow {}^6H_{9/2}$ at ~3.7 µm and $^6H_{11/2} \rightarrow {}^6H_{7/2}$ at~ 4.1 µm; each has a similar branching ratio [15]. Emission from ($^6F_{1/2}$, $^6F_{3/2}$, $^6H_{15/2}$) $\rightarrow {}^6H_{11/2}$ at ~ 4.03 µm (branching ratio 0.06 [15]) may contribute, despite the low branching ratio.

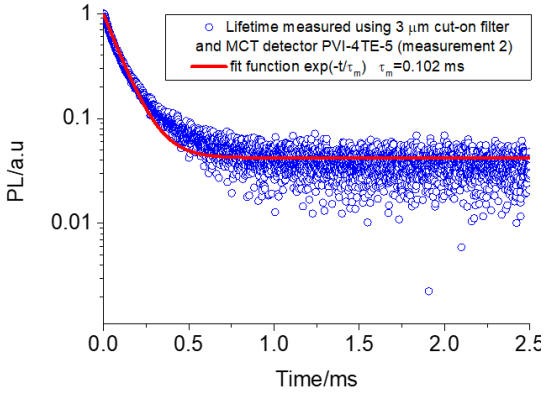

Fig. 7. Photoluminescent lifetime of 1000 ppmw Sm^{3+}-doped $(GeSbSe)_{97}Ga_3$ glass centered at 3.75 µm (see Fig. 5(a)) with cut-on filter at 3.00 µm and fiber-side collection. Typical measurement, 2nd of 3 measurements; in order to suppress noise, averaging over several thousand excitation processes per measurement was performed.

(ii) PL decay centered at 7.25 µm, cut-on filter at 6.15 µm, fiber-side collection

Fig. 8 presents the PL decay of the of the 1000 ppmw Sm^{3+}-doped $(GeSbSe)_{97}Ga_3$ glass fiber using the MCT detector (PVI-4TE-8) and cut-on filter at 6.15 µm; the PL was centered at 7.25 µm (see Fig. 5(b)). As low pump power as possible was used in order to minimize heating of the sample. The decay was measured from the fiber-side. The measured lifetime was fitted using a single exponential function. The calculated PL lifetime was in the range of 0.1 ms; measurements were repeated 3 times: 0.0975 ms, 0.0971 ms and 0.104 ms. A single exponential was fitted, but was not a perfect fit. It is suggested that this is because there is more than one transition contributing: $^6H_{13/2} \rightarrow {}^6H_{9/2}$ at around 7.25 µm and $^6H_{11/2} \rightarrow {}^6H_{9/2}$ at around 7.8 µm; these two transition have a similar branching ratio [15]. Also, emission from ($^6F_{1/2}$, $^6F_{3/2}$, $^6H_{15/2}$) $\rightarrow {}^6H_{11/2}$ may contribute to the MIR emission but this has a low branching ratio [15].

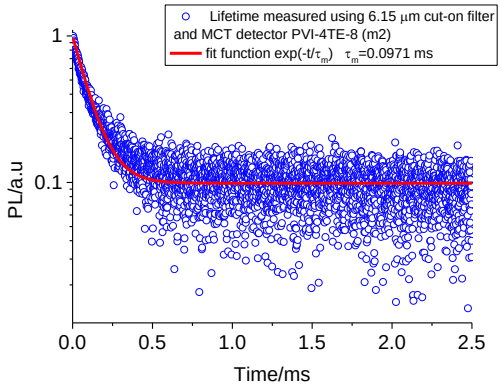

Fig. 8. Photoluminescent lifetime of 1000 ppmw Sm^{3+}-doped $(GeSbSe)_{97}Ga_3$ glass centered at 7.25 µm with cut-on filter at 6.15 µm measurement (2nd of 3 measurements, in order to suppress noise, averaging over several thousand excitation processes per measurement was performed).

4. Discussion

4.1 Development of low optical loss host glass system for long wavelength

The much-investigated host glass system GeAsSeGa is a current benchmark for rare earth ion doped chalcogenide glass fibers. Fiber losses as low as 1.16 dB/m at 6.56 µm have been measured for Dy^{3+} doped glass [26] with others reporting losses of 2-3 dB/m [27-29]. To the Authors' knowledge, no emission beyond the 3.5-6 µm wavelength range exhibited by Pr^{3+} has been recorded from a GeAsSeGa fiber [29, 30]. Accessing longer wavelength rare earth ion emissions may therefore require the development of active chalcogenide fibers of comparatively lower phonon energy. $Ga_5Ge_{20}Sb_{10}Se_{65}$ at. % fibers doped with 500 ppmw Tb^{3+} has facilitated 8 µm emission, with a background loss of 2.5 dB/m [14]. 2000 ppmw Pr^{3+} $Ge_{15}As_{16}Se_{63}In_3I_3$ at. % and 500 ppmw Pr^{3+} GeAsInSe fibers have been fabricated with losses *ca.* 1 dB/m, and 4.3 dB/m, respectively [27,28]. The low loss of the former fiber can be attributed to an intricate distillation process. Despite being comprised of lower phonon energy constituents, no emission beyond 6 µm was measured from these fibers. The fiber reported herein exhibited a fiber loss to rival the GeAsSeGa system (2.15 dB/m at 6.04 µm) while also facilitating longer wavelength (7.3 µm) emission.

4.2 Fiber PL and PL lifetime

Pumping with 1300 nm into the $^6F_{7/2}$ level resulted in a less intense emission despite the increase in pump power when compared to pumping at 1470 nm. Yet the $^6F_{7/2}$ has a higher absorption coefficient of 0.72 cm^{-1} at 1300 nm, whilst that of the $^6F_{5/2}$ manifold was 0.58 cm^{-1} at 1470 nm. The disparity in emission intensity may be explained by the lower quantum efficiency when pumped at 1300 nm.

To the Authors' knowledge, this Paper reports the first decay lifetime measured for a Sm^{3+} doped chalcogenide fiber at 7.25 µm. Judd-Ofelt analysis for a similar host glass in [15] predicted a ~4.3 ms lifetime, however, the measured lifetime (~ 0.1 ms) here was considerably faster, yet similar to that found for Dy^{3+} at 7 µm (~43 µs) [31]. The Authors of [15] commented on the unlikelyhood of a Sm^{3+} $^6H_{13/2} \rightarrow {}^6H_{11/2}$ radiative emission at 7.77 µm (Fig.5) due to its small energy gap, yet it is suggested in the current work that this emission is indeed active.

5. Conclusions

1000 ppmw Sm^{3+}-doped $(GeSbSe)_{97}Ga_3$ glass was successfully drawn to an unstructured fiber with minimum loss of 2.15 dB/m at 6.04 µm wavelength. The fiber provided emission in the 3.25-4.5 µm and 6.23-9 µm wavelength range when pumped with 1300 nm or 1470 nm laser diodes. The first recorded Sm^{3+} lifetime at 7.25 µm was measured to be 0.1 ms.

6. Funding, acknowledgments, and disclosures

6.1 Funding

EPSRC (EP/P013708/1) and British Council (Grant Reference 277109657).

6.2 Acknowledgments

The Authors thank the Engineering & Physical Sciences Research Council, UK, [EP/P013708/1] Project: COOL (COld-cOntainer processing for Long- wavelength mid-infrared fiberoptics) and the British Council (Ref. 277109657) for funding support.

6.3 Disclosures

The authors declare no conflicts of interest.

References

1. BSI ISO, *20473:2007 Optics and Photonics — Spectral Bands* (British Standards Institution (BSI), 2015).
2. J. Hodgkinson, R. P. Tatam, "Optical gas sensing: A review", Meas. Sci. Technol. **24,** 012004 1-59 (2013).
3. B. M. Walsh, H. R. Lee, and N. P. Barnes, "Mid-infrared lasers for remote sensing applications", J. Lumin. **169**, 400–405 (2016).
4. A. B. Seddon, "Biomedical Applications in Probing Deep Tissue using Mid-Infrared (MIR) Supercontinuum Optical Biopsy" in Deep Imaging in Tissue and Tissue-Like Media with Linear and Nonlinear Optics], eds. Alfano, R. R., Shi. L., Pan Stanford Publishing, Singapore, printed in GB. 2017.
5. V. A. Serebryakov, É. V. Boĭko, N. N. Petrishchev, and a. V. Yan, "Medical applications of mid-IR lasers

problems and prospects", J. Opt. Technol. **77**(1), 6-17 (2010).
6. A. B. Seddon, "Mid-infrared (IR) - A hot topic: The potential for using mid-IR light for non-invasive early detection of skin cancer in vivo", Phys. Status Solidi Basic Res. **250**, 1020–1027 (2013).
7. C. R. Petersen, U. Møller, I. Kubat, B. Zhou, S. Dupont, J. Ramsay, T. Benson, S. Sujecki, N. Abdel-Moneim, Z. Tang, D. Furniss, A. Seddon and O. Bang, "Mid-infrared supercontinuum covering the 1.4–13.3 μm molecular fingerprint region using ultra-high NA chalcogenide step-index fiber, Nature Photonics", **8**, 830–834 (2014).
8. A. B. Seddon, Z. Tang, D. Furniss, S. Sujecki and T. M. Benson**,** "Progress in rare-earth-doped mid-infrared fiber lasers", Opt. Exp**. 18**(25), 26704-26719 (2010).
9. S. D. Jackson, "Towards high-power mid-infrared emission from a fiber laser", Nat. Photonics **6**, 423–431 (2012).
10. O. Henderson-Sapir, S. D. Jackson, and D. J. Ottaway, "Versatile and widely tunable mid-infrared erbium doped ZBLAN fiber laser", Opt. Lett. **41**(7), 1676-1679 (2016).
11. F. Maes, V. Fortin, S. Poulain, M. Poulain, J.-Y. Carrée, M. Bernier, and R. Vallée, "Room-temperature fiber laser at 3.92 μm", Optica **5**(7), 761-764 (2018).
12. J. Ari, F. Starecki, C. Boussard-Plédel, Y. Ledemi, Y. Messaddeq, J.-L. Doualan, A. Braud, B. Bureau and V. Nazabal, "Co-doped Dy^{3+} and Pr^{3+} $Ga_5Ge_{20}Sb_{10}S_{65}$ fibers, for mid-infrared broad emission", Opt. Lett. **43**, 2893-2896 (2018).
13. X. Xiao, Y. Xu, J. Cui, X. Liu, X. Cui, X. Wang, S. Dai and H. Guo, "Structured active fiber fabrication and characterization of a chemically high-purified Dy^{3+}-doped chalcogenide glass", J Am Ceram Soc. 00 1–11 (2019). DOI: 10.1111/jace.16921
14. F. Starecki, N. Abdellaoui, A. Braud, J.-L. Doualan, C. Boussard-Plédel, B. Bureau, P. Camy, and V. Nazabal, "8 μm luminescence from a Tb^{3+}GaGeSbSe fiber", Opt. Lett. **43**, 7–10 (2018).
15. F. Starecki, A. Braud, N. Abdellaoui, C. Boussard-plédel, B. Bureau, and V. Nazabal, "7 to 8 μm emission from Sm^{3+} doped selenide fibers", Opt. Express **26**, 26462–26469 (2018).
16. P. Němec, J. Oswald, M. Frumar and B. Němecova, "Optical propertie of germanium-gallium-selenium glasses doped by samarium", J. Optoelect. Adv. Mat. **1**(4), 33-41 (1999).
17. M.C. Farries, P.R. Morkel and J.E. Townsend, "Samarium^{3+} -doped glass laser operating at 651 nm", Electr. Lett. **24**(11), 709-710 (1988).
18. D. Furniss and A. B. Seddon, Chapter 10: "Thermal analysis of inorganic compound glasses and glass ceramics", in Principles and Applications of Thermal Analysis, Editor Paul Gabbott, Wiley-Blackwell (2007) ISBN: 978-1-405-13171-1.
19. Z. Tang, V. S. Shiryaev, D. Furniss, L. Sojka, S. Sujecki, T. M. Benson, A. B. Seddon, and M. F. Churbanov, "Low loss Ge-As-Se chalcogenide glass fiber, fabricated using extruded preform, for mid-infrared photonics", Opt. Mater. Express **5**(8), 1722-1737 (2015).
20. Y. Fang, D. Furniss, D. Jayasuriya, H. Parnell, R. Crane, Z. Q. Tang, E. Barney, C. L. Canedy, C. S. Kim, M. Kim, C. D. Merritt, W. W. Bewley, I. Vurgaftman, J. R. Meyer, A. B. Seddon and T. M. Benson, "Determining small refractive index contrast in chalcogenide-glass pairs at mid-infrared wavelengths", Opt. Mat. Exp. **9**(5), 2022-2026 (2019).
21. F. Starecki, A. Braud, J.-L. Doualan, J. Ari, C. Boussard-Plédel, K. Michel, V. Nazabal, and P. Camy, "All-optical carbon dioxide remote sensing using rare earth doped chalcogenide fibers", Optics and Lasers in Engineering **122**, 328–334 (2019).
22. H. Parnell, D. Furniss, Z. Q. Tang, N. C. Neate, T. M. Benson and A. B. Seddon, "Compositional-dependence of crystallization in Ge–Sb–Se glasses relevant to optical fiber making", J. Am. Ceram. Soc. **101**(1), 208-219 2018.
23. D. W. Sheibley and M. H. Fowler, "Infrared spectra of various meta oxides in the region of 2 to 26 microns", NASA (National Aeronautics and Space Administration] Technical Note 03, (1966). https://ntrs.nasa.gov/search.jsp?R=19670003469 2019-11-08T20:45:40+00:00Z
24. C.T. Moynihan, P.B. Maklad, M.S. Mohr and R.E. Howard, "Intrinsic and impurity infrared-absorption in As_2Se_3 glass", J. Non-Cryst. Solids **17** 369-385 (1975).
25. J. A. Savage, P. J. Webber and A. M. Pitt, "The potential of Ge-As-Se-Te glasses as 3-5 μm and 8-12 μm infrared optical materials", Infrared Physics **20** 313-320 (1980).
26. Z. Tang, D. Furniss, M. Fay, N. C. Neate, S. Sujecki, T. M. Benson, and A. B. Seddon, "Crystallization and Optical Loss Studies of Dy^{3+} -Doped, Low Ga Content, Selenide Chalcogenide Bulk Glasses and Optical Fibers", in *Processing, Properties, and Applications of Glass and Optical Materials* (The American Ceramic Society), 193–199 (2012).
27. H. Sakr, D. Furniss, Z. Tang, L. Sojka, N. A. Moneim, E. Barney, S. Sujecki, T. M. Benson, and A. B. Seddon, "Superior photoluminescence (PL) of Pr $^{3+}$-In, compared to Pr^{3+}-Ga, selenide-chalcogenide bulk glasses and PL of optically-clad fiber", Opt. Express **22**, 21236-21252 (2014).
28. E. V. Karaksina, V. S. Shiryaev, M. F. Churbanov, E. A. Anashkina, T. V. Kotereva, and G. E. Snopatin, "Core-clad Pr^{3+}-doped Ga(In)-Ge-As-Se-(I) glass fibers: Preparation, investigation, simulation of laser characteristics", Opt. Mater. **72**, 654–660 (2017).
29. Z. Tang, D. Furniss, M. Fay, H. Sakr, L. Sójka, N. Neate, N. Weston, S. Sujecki, T. M. Benson, and A. B. Seddon, "Mid-infrared photoluminescence in small-core fiber of praseodymium-ion doped selenide-based chalcogenide glass", Opt. Mater. Express **5**, 870-886 (2015).

28 L. Sójka, Z. Tang, D. Furniss, H. Sakr, A. Oladeji, E. Bereś-Pawlik, H. Dantanarayana, E. Faber, A. B. Seddon, T. M. Benson, and S. Sujecki, "Broadband, mid-infrared emission from Pr^{3+} doped GeAsGaSe chalcogenide fiber, optically clad", Opt. Mater. **36**, 1076–1082 (2014).

29 F. Starecki, G. Louvet, J. Ari, A. Braud, J.-L. Doualan, R. Chahal, I. Hafienne, C. Boussard-Plédel, V. Nazabal, and P. Camy, "Dy^{3+} doped GaGeSbSe fiber long-wave infrared emission", Journal of Luminescence **218**,116853 (2020). https://www.sciencedirect.com/science/article/pii/S0022231319314721